Chemical Engineering Journal 435 (2022) 135076

Contents lists available at ScienceDirect

Chemical Engineering Journal

journal homepage: www.elsevier.com/locate/cej

Using copper-based biocathodes to improve carbon dioxide conversion efficiency into methane in microbial methanogenesis cells

Gahyun Baek, Le Shi, Ruggero Rossi, Bruce E. Logan *

Department of Civil and Environmental Engineering, The Pennsylvania State University, 231Q Sackett Building, University Park, PA 16802, USA

ARTICLE INFO

Keywords:
Biocathodes
Carbon dioxide conversion
Electromethanogenesis
Methane
Copper electrode

ABSTRACT

Copper can be used as a metal catalyst for abiotic CO_2 conversion into methane and organic chemicals, but it has not been examined as a catalyst for enhancing biotic methane generation in microbial methanogenesis cells (MMCs). In this study, copper-based electrodes prepared using several different techniques were compared to the performance of MMCs containing graphite block cathodes. Gas production was examined under both abiotic and biotic conditions at a fixed cathode potential of –0.9 V vs. Ag/AgCl in two-chamber electrochemical cells. All copper-based cathodes showed better methane production than plain graphite blocks except for the cathode made from copper foil which lacked a biocompatible surface. The cathode prepared by an electroless Cu deposition (electroless-Cu) method had the highest current density production of 0.6 A/m^2 and methane production rate of 201 nmol/cm^3/d, and its performance was stable over time. Both the electroless-Cu and electrodeposited Cu electrodes produced more current than that obtained with copper powders with a Nafion binder (Nafion-Cu), likely due to different surface characteristics such as hydrophobicity and uniformity of the copper layer. The results of this study showed that copper-based biocathodes improved methane production relative to plain graphite materials and techniques for preparing copper electrodes impact bioelectrochemical performance with the highest performance in the electroless-Cu reactors.

1. Introduction

Carbon capture and utilization (CCU) technologies are being examined as methods to address climate change by producing valuable products from CO_2. The electrochemical conversion of CO_2 into methane (CH_4) could be a particularly useful method for producing a biofuel combined with a renewable energy source as long as CH_4 is not released into the atmosphere during the process [1]. The electrochemical conversion of CO_2 to other chemical forms requires a high over potential of cathode due to stable structure of CO_2 and it can be limited by low solubility and ineffective mass transfer of CO_2 into solution [2]. Electromethanogenesis is a biological process that uses microorganisms as biocatalysts on the cathode to minimize overpotentials for biological conversion of CO_2 into methane [3]. In microbial methanogenesis cells (MMCs), electromethanogenesis takes place on the cathode using electrons generated from anodic reactions such as water splitting in abiotic anodes or organics oxidation by biotic anodes depending on the experimental conditions. When the goal of the bioelectrochemical system is to produce primarily organic chemicals such as acetate and formate these systems are referred to as microbial electrosynthesis (MES) cells [4]. Since the goal here was to produced methane we refer to this system as an MMC despite the possibility of production of additional organic chemicals. The enriched biocathodes in MMCs provide several advantages over abiotic CO_2 reduction reactions such as high selectivity of final products, high theoretical energy conversion efficiencies, and reduced overpotentials [5]. Methanogens on the cathode can produce methane by several different methods including direct electron transfer, using chemical products such as hydrogen gas released by biotic or abiotic reactions, and chemicals produced by the cathode such as formate by abiotic reactions or released enzymes [6,7].

Most MMC reactors have used carbon-based materials for the biocathodes to enhance direct electron transfer to methanogens while avoiding H_2 generation and the need for precious metals such as platinum. These carbon materials include graphite felt, cloth, plates, and brushes [8–11] that have a relatively low cost and can be highly biocompatible for biofilm formation. Non-precious metal catalysts can also be used for abiotic electrochemical CO_2 conversion into products other than H_2 due to their high electrocatalytic activity. According to the

* Corresponding author.
E-mail address: blogan@psu.edu (B.E. Logan).

https://doi.org/10.1016/j.cej.2022.135076
Received 30 November 2021; Received in revised form 14 January 2022; Accepted 31 January 2022
Available online 5 February 2022
1385-8947/© 2022 Elsevier B.V. All rights reserved.

Sabatier principle, the catalytic activity of a metal catalyst depends on the binding energy between the catalyst and the reactant [12]. If the interaction between the two is too weak, the reactant will fail to bind to the catalyst surface and if it is too strong the product will fail to dissociate [13]. Based on this principle, copper (Cu) has been found to be a suitable non-precious metal catalyst for abiotic CO_2 conversion to reduced forms other than H_2 owing to its good catalytic activity indicated in the volcano plot for the CO_2 reduction reaction [14]. Copper-catalyzed electrodes can abiotically convert CO_2 into methane and carbon monoxide, but they also can be used to produce organic chemicals including formate, ethanol, methanol, and acetate, which can be good substrates for certain methanogens [15–17].

There are two additional points to be considered in this study to adopt copper-based materials as biocathodes for MMCs: biofilm formation on the electrode surface, and CO_2 conversion under typical cathodic potentials. Despite good electrical conductivity and catalytic activities, many metals such as copper may not provide a good surface for microbial adhesion which could limit development of a thick biofilm on their surface [18,19] although some studies have shown that exoelectrogens can successfully grow on copper [20]. One way to overcome possible biofilm formation limitations is by depositing the metal catalysts on surfaces good for biofilm formation such as carbon-based materials. There are several methods to coat metals on the substrate materials such as electrodeposition, electroless plating, and binding metal particles using polymers. While copper can be used to abiotically produce chemicals from CO_2, the cathodic potentials used for abiotic CO_2 reduction reaction are typically much more negative than those in MMC studies. For example, abiotic CO_2 reduction experiments using copper cathodes were conducted over a range of –1.4 to –1.8 V (versus Ag/AgCl) at a pH of 6.8 [15]. In a study by Kuhl et al. (2012), CO_2 was converted into CH_4 with a comparable current efficiency for H_2 production at cathode potential more negative than –1.7 V vs. Ag/AgCl [15]. This potential is much more negative than that commonly used in in MMCs of –0.7 to –1.1 V vs Ag/AgCl [11]. Therefore, it is not clear if a biocatalyst on a copper electrode could produce better performance than carbon materials in MMCs under cathode potentials typically more positive than –1.7 V vs Ag/AgCl.

In this study, MMC performance was examined in terms of current, methane production rate, and stability for CO_2 reduction using several different copper-based cathode materials. Three different coating methods were used to coat copper on graphite electrodes, and their biotic and abiotic performance were compared with those of pure copper and plain graphite electrodes. The electrochemical and physical properties of each electrode were evaluated and then compared to MMC performance based on biogas generation rates.

2. Materials and methods

2.1. Cathode preparation

Plain graphite blocks (2 cm × 2 cm × 0.32 cm, McMaster-Carr, Cleveland, OH) were used as a control material, or they were coated with copper using three different methods. Graphite blocks were drilled to make two holes of 0.8 mm diameter to insert a titanium wire through the top hole and then bent around in a J-shape into the second hole to make a good electrical connection [21]. The blocks were polished using sandpaper, sonicated in acetone for 20 min, immersed in 1 N HCl overnight, and then rinsed with deionized water. The three different methods used to coat copper on graphite block were: electrodeposition (e-deposited-Cu), electroless plating (electroless-Cu), and binding copper powders with a polymer (Nafion) binder (Nafion-Cu) (Fig. 1). The electrodeposition process was conducted using a copper mesh anode (wire thickness, 0.6 mm; opening size, 0.2 cm; 2 cm × 2 cm) and a graphite block cathode. A fixed voltage of 1 V between anode and cathode was applied for 10 min in the electrolyte consisting of 32 g/L $CuSO_4$ in 150 g/L of H_2SO_4 solution [22]. To perform electroless plating of copper the block was first immersed in the sensitization solution (30 g/L $SnCl_2$, 60 mL/L HCl) for 15 min, followed by transfer into the activation solution (0.25 g/L $PdCl_2$, 10 mL/L HCl) for 15 min. The blocks were then immersed in the electroless copper solution (32 g/L $CuSO_4$, 15 g/L EDTA disodium, 20 g/L sodium potassium tartrate, 12 g/L NaOH, 0.2 mL/L thiourea, 13 mL/L formaldehyde) at 45 °C and a pH of 12.5 for 20 min [23]. All the obtained electrodes by electrodeposition and electroless plating were washed with deionized water to remove any residual chemicals and loosely bound copper and dried overnight. The Nafion-Cu cathode was made by coating a catalyst slurry consisting of copper powders (10–25 μm; 10% w/w) with carbon black powders (Vulcan XC72) using borosilicate glass balls and a vortexer [10]. The coating slurry was made by adding 0.83 μL of DI water, 6.67 μL of Nafion in an unspecified mix of alcohols (5% w/v) and 3.33 μL of 2-propanol per mg of powder mix. The slurry was applied to the graphite block using a paintbrush and air-dried overnight.

Three different pure copper electrodes, copper foil (0.5 mm of thickness), copper mesh (wire thickness, 0.6 mm; opening size, 0.2 cm), and copper cloth (wire thickness, 0.2 mm; opening size, 0.2 mm), were cut into the same projected surface area as graphite block (2 cm × 2 cm) (Fig. 1). The mass of copper was determined by directly weighing electrodes (for pure copper electrodes) or by calculating the difference in mass before and after copper coating on the graphite block (for copper-coated electrodes) (Fig. S1). Total surface area was calculated by sum of six faces of electrodes except for copper mesh and cloth which

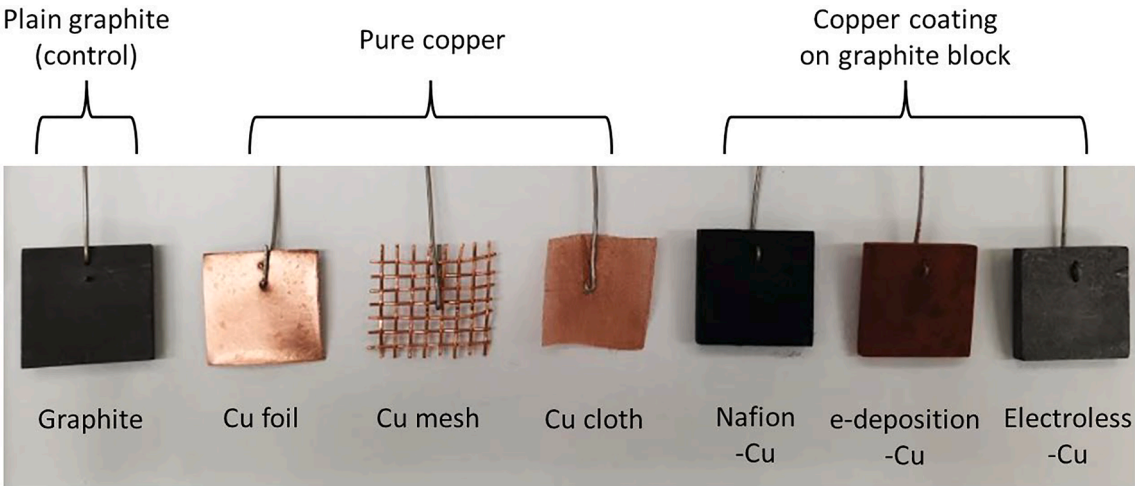

Fig. 1. Photographs of seven different biocathodes used in this study.

was calculated following previous study (Fig. S1) [24]. All electrodes used in this study had a contact resistance <1.0 Ω after connecting with titanium wires.

2.2. Reactor construction and operation

Two-chamber reactors were constructed by separating the side arms (inner diameter 2.4 cm; length 3.8 cm) of two glass bottles with a proton exchange membrane (PEM, Nafion 117; Fuel Cell Store, CO) held in place using an O-ring and screw clamp. The bottles were filled with either 100 mL (biotic tests) or 110 mL (abiotic tests) of the medium. The anodes were carbon brushes (4 cm long and 4 cm in diameter) made using carbon fibers wound into two twisted titanium wires [10]. The carbon brushes were heat treated at 450 °C for 30 min before use. The carbon-based anode was used here due to its low cost, but overall efficiencies could be improved by using IrO_2 catalysts on the anodes [25]. The reference electrodes (Ag/AgCl electrode; 3 M of KCl) were inserted into the cathode chamber through a hole in the rubber stopper that was used to seal the bottles. All potentials were reported here versus a Ag/AgCl reference electrode (+200 mV vs. a standard hydrogen electrode, SHE). Tests were performed in duplicate. Reactors were operated at 30 °C in the dark. The current was recorded at 10 min intervals using a potentiostat (VMP2, BioLogic, Knoxville, TN).

The reactors were operated at fixed cathode potential of –0.9 V which is in the range of typically applied potential in previous MMC studies [26–29] as it is sufficientsu to convert carbon dioxide into methane via both direct and indirect pathways. A fixed cathode potential was applied to all reactors throughout the operational period except for the open-circuit reactors (Control-OC). Both chambers were filled with the medium containing $NaHCO_3$ (2.5 g/L), NH_4Cl (1.5 g/L), NaH_2PO_4 (0.6 g/L), KCl (0.1 g/L), vitamin (10 mL/L) and mineral solution (10 mL/L) [10]. The pH of the medium was adjusted to 7.0 before use and no further pH adjustments were made during operation. The medium was sparged with CO_2/N_2 (20:80 v/v) gas for 10 min before every new cycle to provide CO_2 and remove residual gas in the solution from previous cycles. The carbon source for methanogenesis was provided by both forms of bicarbonate in the medium and CO_2 gas in the headspace to minimize substrate limitations for microbial metabolism.

Biocathodes were first enriched in a single chamber microbial electrolysis cell configuration [9] using graphite blocks as the anodes and a sludge inoculum 50% (v/v) from the anaerobic digester at the Pennsylvania State University wastewater treatment plant at an applied voltage of 1.0 V. The anaerobic sludge composition was: total chemical oxygen demand (TCOD) of 17,700 ± 200 mg/L, soluble COD (SCOD) of 408 ± 3 mg/L, total solids (TS) of 37,000 ± 6000 mg/L, total volatile solids (TVS) of 27,500 ± 4000 mg/L, total suspended solids (TSS) of 33,000 ± 0 mg/L, and a volatile suspended solid (VSS) of 25,000 ± 0 mg/L. The medium was the same as that used in the two-chamber MMC reactors except sodium acetate (2 g/L) was added as an organic carbon source for the bioanode. After 2 months of repeated batch operation with 50% of medium replenishment, the biocathodes were transferred to two-chamber MMC reactors for biotic experiments. Five repeated batch cycles (5 days per cycle) were conducted with a complete medium replacement (100%) by fresh one for both anolyte and catholyte at the beginning of each cycle.

2.3. Material characterization and electrochemical analyses

Electrodes were examined using scanning electron microscopy (SEM) Verios G4 SEM (Thermofisher-Scientific, Hillsboro, OR) and energy dispersive X-ray spectroscopy (EDS) mapping was performed using an X-MaxN EDS detector (Oxford Instruments, Concord, MA) with an accelerating voltage of 15 keV. To estimate electrochemically active surface area (ECSA) of each cathode material, the electrochemical double-layer capacitance (C_{dl}) was measured through cyclic voltammetry (CV) with different scan rates ranging from 60 to 140 mV/s [30]. The small potential range (–0.85 to –0.95 V) was used to obtain CV results. Current density was calculated as $J = 0.5 \times (J_a - J_c)$, where J_a and J_c indicated the anodic and cathodic current densities recorded at –0.9 V. The slope of linear relationship between current density and scan rate was determined as the C_{dl} value, which is proportional to the ECSA [30]. Linear sweep voltammetry (LSV) experiments were conducted under abiotic conditions before batch tests using a potential range of–0.4 to –1.7 V and a scan rate of 10 mV/s. The LSV was performed to investigate the electrochemical efficiency of each cathode material by overpotential for current production.

2.4. Chemical analyses

Gas composition was analyzed using a gas chromatograph (GC) by extracting 250 μL of gas from the headspace using an airtight gas syringe (Hamilton, Reno, NV, USA). Hydrogen and methane were analyzed using a GC (model 2601B, SRI Instrument, Torrance, CA, USA) equipped with a 3-m Molsieve 5A 80/100 column (Altech Associates, Inc., Bannockburn, IL, USA) and thermal conductivity detector (TCD) with argon as the carrier gas. Carbon dioxide was analyzed using another GC (model 310, SRI Instrument, Torrance, CA, USA) with a 1-m silica gel column (Restek, Bellefonte, PA, USA) and TCD with helium as the carrier gas.

Formate and acetate were measured with high performance liquid chromatography (HPLC; CTO-20A UFLC; Shimadzu, Columbia, MD) equipped with an autosampler (model SIL-20A HT, Shimadzu, Columbia, MD) and column (250×4.6 mm "Allure Organic Acids", 5 μm particle size; Restek, Bellefonte, PA). Propionate, and butyrate were measured using a GC (Shimadzu, GC-2010 Plus, Japan) equipped with a Stabilwax-DA column (30 m × 0.32 mm × 0.5 μm, Restek, Bellefonte, PA) and flame ionization detector (FID; a detection limit of each VFA of 0.1 mM) with nitrogen as the carrier gas. The samples were prepared by using a syringe filter with 0.45 μm of pore size. Total inorganic carbon (TIC) concentration was quantified by infrared detection after persulfate oxidation using total organic carbon analyzer (TOC-VCSN, Shimadzu Co., Kyoto, Japan). The solution pH was measured using a probe (SevenMulti, Mettler-Toledo International Inc.) and meter (SevenMulti, Mettler Toledo, OH).

3. Results & discussion

3.1. Characterization of cathode materials

The ECSA of each cathode material was estimated based on the C_{dl} (Fig. 2 and Fig. S2). Although all materials had an identical projected surface area (4 cm^2), the ECSA values can be substantially affected by microstructure of the materials so it could give more comprehensive insight on the potential electrochemical performance of them as electrodes [31]. The C_{dl} was higher for the plain graphite (1.12 mF/cm^2) and Nafion-Cu (1.11 mF/cm^2) electrodes, followed by electroless-Cu (0.79 mF/cm^2), e-deposition-Cu (0.69 mF/cm^2), and Cu foil (0.09 mF/cm^2) electrodes. The differences in the C_{dl} of the materials were likely due in part to the different surface morphology of each material as shown by the analysis using the SEM (Fig. S3). The plain graphite block had a rough surface with some irregular pores compared to other materials, which could enlarge its ECSA even with the same projected surface area [32]. In contrast, the Cu foil had a very smooth surface, typical of many pure metal surfaces [18]. The copper-based cathodes prepared by different methods had appreciably different surface morphologies. The copper layers formed using the Nafion binder or electrodeposition seemed to be smoother than the original rough and porous surface of the plain graphite block. A smoother surface could reduce the active electrode area. However, the Nafion-Cu electrodes had much smaller particles than e-deposition-Cu electrodes, which may have compensated for the surface area reduction by the production of many smaller particles consistent with the results that these electrodes had a high electrochemically active surface area.

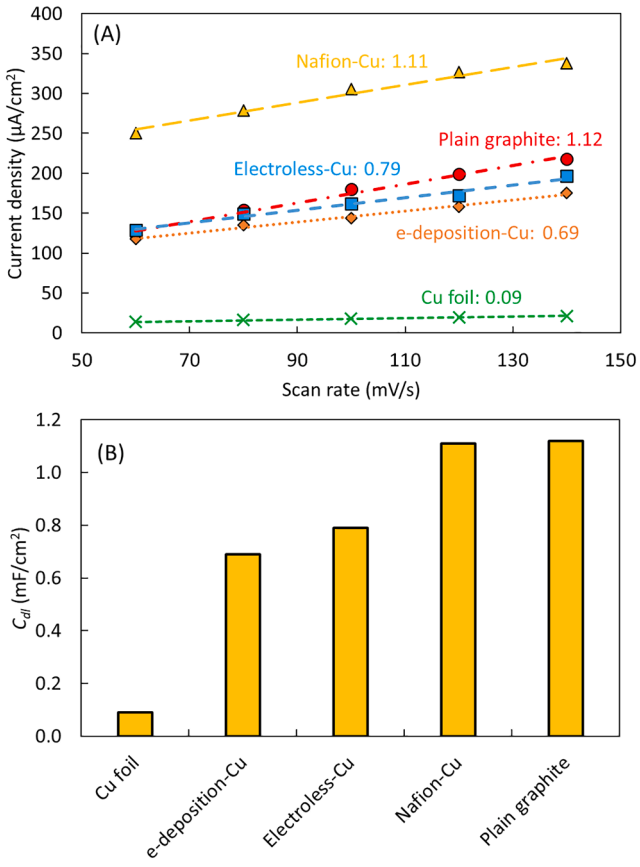

Fig. 2. (A) Current density as a function of scan rates where the numbers indicate the slope of the trendline and (B) electrochemical double-layer capacitance (C_{dl}) calculated from the slope of the relationship between current density and scan rate. The current density was obtained from the cyclic voltammetry (CV) curves withing the potential range was –0.85 to –0.95 V vs. Ag/AgCl. Current density was calculated as $J = 0.5 \times (J_a - J_c)$, where J_a and J_c indicated the anodic and cathodic current densities recorded at –0.9 V vs. Ag/AgCl.

The relative amounts of copper estimated by EDS surface mapping showed good agreement with the copper mass measured during the preparation processes (Fig. S1). The e-deposition-Cu electrodes had the highest amount of copper on the surface (87 wt%), followed by electroless-Cu (1.2 wt%) and Nafion-Cu (0.8 wt%) (Fig. S4). The electroless-Cu and Nafion-Cu electrodes had similar amounts of copper, but the copper layer appeared to be more uniformly applied on the surface for the electroless-Cu electrode compared to the relatively uneven distribution of copper for the Nafion-Cu material.

3.2. Current and gas production under abiotic conditions

All copper-based cathode materials showed better electrochemical performance than plain graphite block based on the LSVs in abiotic condition (Fig. 3). The LSV using copper-based cathodes showed higher current production compared to that obtained with a plain graphite electrode at the same cathode potential. For example, at cathode potential of –1.7 V, pure copper electrodes (Cu foil, Cu mesh, and Cu cloth) and Nafion-Cu electrode produced >4.5 mA/cm^2 while plain graphite electrodes produced only 2.6 mA/cm^2. The electroless-Cu and e-deposition-Cu electrodes showed much higher current density at the same cathode potential as well as smaller onset potential for increasing current density. The current from the electroless-Cu started to increase when potentials were more negative than –0.7 V and current production was already highest from the e-deposition-Cu electrodes at the lowest

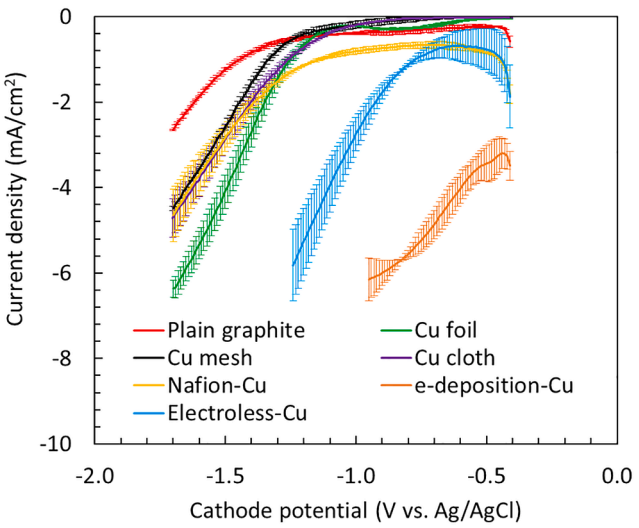

Fig. 3. Electrochemical characterization of copper-based cathode materials through linear sweep voltammograms (LSV) and comparison with plain graphite block used as a control. The current density was normalized by project surface area of each electrode.

scanned voltage (–0.4 V), while other cathodes started to produce current at more negative potential than –1.1 V.

Constant applied voltage tests were conducted to determine abiotic gas production under conditions typical for MMC tests. Each cathode was poised at –0.9 V (for 24 h, with intermittent measurement of gas and liquid concentrations (Fig. 4). Only Cu foil was used as a pure copper electrode due to the similarity of its performance to other copper metal electrodes in LSV tests. Differences in electrocatalytic activities were due to hydrogen gas production since no other gaseous or liquid product

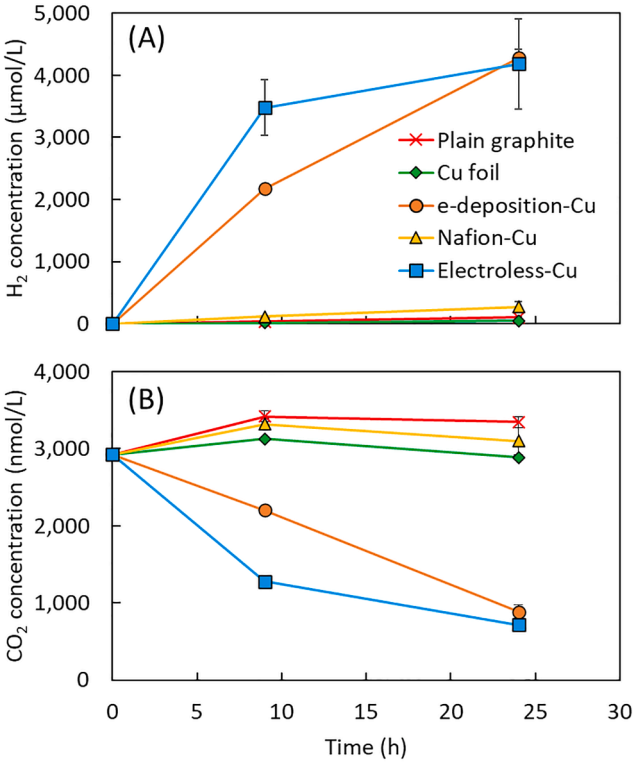

Fig. 4. Changes in concentration of (A) hydrogen and (B) carbon dioxide in the headspace during 24-h abiotic tests. No methane was detected during the experiment.

(methane or VFAs) were detected. The e-deposition-Cu and electroless-Cu cathodes showed highest hydrogen production (4190–4280 μM), followed by Nafion-Cu cathode (273 ± 86 μM), and a negligible H_2 evolution from plain graphite (33 ± 5 μM) and Cu foil (12 ± 0 μM) (Fig. 3A). The results obtained from abiotic tests indicate that there was a clear difference between copper-based electrodes and plain graphite at –0.9 V of cathodic potential, which is in a typical potential range of MMC operation but rarely used in the abiotic CO_2 conversion experiments [26–29]. In addition, each copper-based material showed different electrochemical efficiencies depending on their preparation methods. High electrochemical performance of the e-deposition-Cu electrodes was likely due to the greater amounts of copper on the surface. The electroless-Cu electrodes had a lower amount of copper, but its layer was uniformly deposited on the surface, resulting in high electrochemical performance as well.

A decrease in CO_2 concentration in the headspace (Fig. 3B) was not due to its conversion into other products (e.g., methane or VFAs) in this abiotic condition, but instead due to the absorption of CO_2 into the solution due to a change in pH. Theoretically, protons generated by water splitting reaction from the anode should be transported to cathode chamber through PEM to maintain pH balance between the anolyte and catholyte. However, the catholyte pH can increase due to the competition in the transport across the membrane between protons and other cations that are present in the electrolyte such as Na^+ and K^+ [33]. To confirm that CO_2 absorption was occurring, pH and TIC concentrations were monitored after 24 h using plain graphite or electroless-Cu cathodes (Fig. S5). As the pH increased from 7.0 to 8.1 in the electroless-Cu reactors with rapid H_2 production, TIC concentrations in the liquid increased from 343 to 380 mg/L, demonstrating that CO_2 in the headspace was absorbed into the liquid and there was no net consumption of CO_2 or bicarbonate. In contrast, there was negligible pH change and slightly reduced TIC concentration after reaction in the plain graphite reactors, possibly due to lower current production. Because current production was low, pH change was less than the electroless-Cu reactors and thus less CO_2 was absorbed from the headspace to the catholyte. A slightly reduced TIC concentration was possibly due to a saturation of CO_2 between the headspace and solution, supported by a slight increase of CO_2 concentration in the headspace (Fig. 3B). The lack of any electroreduction of CO_2 into other reduced products observed here was different from previous abiotic results showing that CO_2 could be converted to products such as CH_4, methanol, or formate, on metallic copper surfaces [14–16,34]. The reason for a lack of these chemical products was likely the less negative cathodic potentials applied here compared to previous abiotic studies to provide operational conditions appropriate for MMC operation.

3.3. MMC performance with different cathodes

All copper-based electrodes except for the Cu foil showed better methane production than plain graphite electrodes as biocathodes in MMCs (Fig. 5). The electroless-Cu reactors showed the best performance in terms of both methane production rate and stability over cycles, having 110–201 nmol/cm^3/d of methane production rate. The Nafion-Cu reactors had comparable performance to the electroless-Cu reactors during the first two cycles but deteriorated rapidly from the third cycle and reached 8 nmol/cm^3/d at the end of operation. There was negligible methane production (<0.5 nmol/cm^3/d) from both the open circuit control and the Cu foil electrodes, except for small amount produced in the third cycle using the Cu foil, indicating that electron supply and biofilm formation were crucial factors for methane production in MMCs here. Although the Cu foil showed better electrochemical performance than the plain graphite in abiotic LSV tests, it did not effectively produce methane in MMCs. This different observation suggests that poor performance in biotic tests was likely because the Cu foil could not provide enough surface for biomass growth in terms of roughness or porosity compared to other materials observed by SEM images (Fig. S3).

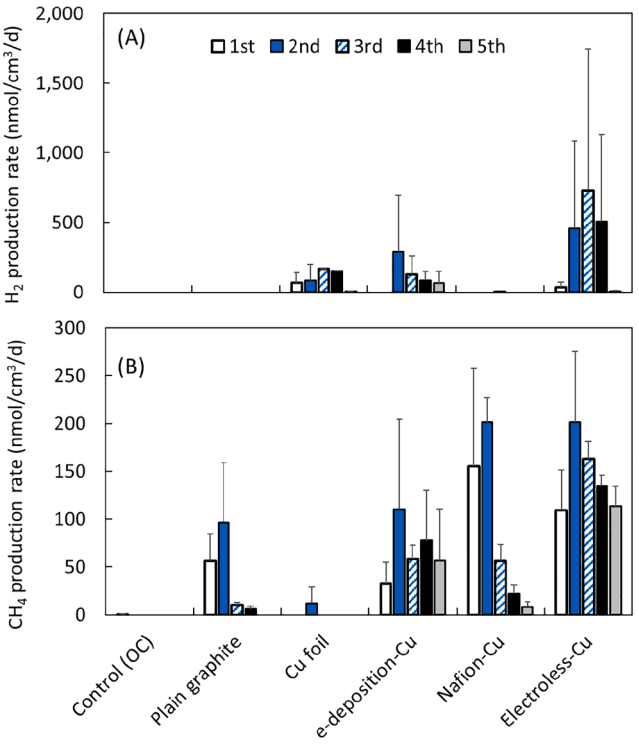

Fig. 5. Rates of (A) hydrogen and (B) methane gas productions from biotic tests during batch cycles 1–5. All experiments were conducted at fixed cathodic potential of –0.9 V vs. Ag/AgCl except for the control reactors operated under open circuit (OC) potential.

The gradual decrease in the methane production rates in the reactors after the second cycle (Fig. 5) was due to corrosion of the carbon brush anode, as evidenced by the development of a dark brown color of the anolyte over time [35] (Fig. S6). In addition, 100% replacement of medium at the end of every cycle may have negatively impacted MMC stability due to insufficient retention time for biomass attachment onto the electrode surface and disturbance of the biofilm on the cathodes. Graphite blocks are particularly susceptible to biofilm loss as their surface area is low, compared to other carbon-based materials such as felt, cloth, and brushes which have interior surfaces [36], so only small changes in biofilm integrity can largely affect MMC performance. Only the e-deposition-Cu and electroless-Cu electrodes maintained their higher methane production until the last cycle, showing 56 nmol/cm^3/d (e-deposition-Cu) and 113 nmol/cm^3/d (electroless-Cu), which is in line with their best performance in abiotic experiments (Fig. 4). However, the methane production rates obtained from this study was lower than previously reported MMC performances (Table S1), likely because carbon brush without any catalyst was used as an anode and H-type cells with high internal resistance were used.

The best MMC performance of the electroless-Cu reactors was attributed to high electrocatalytic activity of this cathode material, as observed from the abiotic results, due to a high ECSA and a uniformly distributed Cu layer on the surface. The stability in performance over multiple cycles indicated that this surface was biocompatible for microbial attachment to the cathode. In contrast, the Cu foil had a very smooth surface with less porosity and roughness compared to other cathode materials as seen in the SEM images (Fig. S4) which could indicate poor biocompatibility consistent with a failure in methane production over time. The low stability of the Nafion-Cu reactors, shown by a decrease in rates of methane over time (from 201 to 8 nmol/cm^3/d), could be due to the partially hydrophobic surface created using the Nafion binder. Nafion has phase-separated structures comprised of hydrophilic ionic clusters and hydrophobic perfluorocarbon backbones

[37]. The presence of hydrophobic regions on the surface of the electrode (i.e., relatively hydrophobic surface compared to other electrodes used here) could limit biofilm formation or decrease stability (detachment) over time [38]. Partially hydrophobic surfaces of the Nafion-Cu electrodes could also have led to the extremely low H_2 production from these reactors (<0.6 nmol/cm^3/d) compared to other copper-based electrodes (Fig. 5A). It was previously reported that hydrophobic surface constructed on copper oxide nanowire electrodes by Nafion coating could enhance the selectivity of CO_2 reduction reaction by suppressing H_2 evolution activity [39]. Overall, copper-based cathodes except for the Cu foil showed better MMC performance compared to the plain graphite. This is possibly due to the high catalytic activity of copper in terms of the interaction between catalyst surface and the reactant as explained by the Sabatier principle and observed in many abiotic experiments [12]. The binding energy for adsorbed reaction intermediates (e.g., carbon monoxide) on copper surface is a key reason for its better ability to catalyze CO_2 reduction to final products which are further reduced form of the intermediates [16].

Total cathodic recoveries in terms of biogas and liquid chemical productions were calculated based on the current produced during each cycle (Fig. 6 and Fig. S7). The total cathodic recovery based on hydrogen, methane, and VFA species (only formate and acetate were detected) production were quite low even for the electroless-Cu reactors (23–60%) which showed the best MMC performance (Fig. 6). There was only a limited production of VFAs during 1–3 cycles except for the Cu foil reactors in the second cycle and the electroless-Cu reactors in the third cycles, showing <0.05 mM of formate and no acetate production and <2% of formate production as cathodic recovery (Fig. S7). In the last cycle the formate concentration was higher in the e-deposition-Cu reactors (0.12 ± 0.01 mM), Cu foil reactors (0.11 ± 0.03 mM), electroless-Cu reactors (0.09 ± 0.05 mM), and Nafion-Cu reactors (0.05 ± 0.06 mM), compared to the plain graphite reactors (no production). Higher formate productions from copper-based cathodes than graphite ones might be related to the observations from the previous abiotic CO_2 conversion study, where formate and hydrogen were the main products from copper at relatively lower overpotential (before reaching −1.4 V vs. Ag/AgCl) [15]. Although the absolute concentration of VFAs were low, our systems can be also referred to as an MES systems as organic acids are biotically produced.

Low total cathodic recovery from MMCs in this study could be attributed to intrinsic disadvantages of graphite block or foil as bioelectrodes to carry enough amount of biomass as well as 100% medium replenishment, leading electron loss to other pathways than gas-producing activities [40]. There are several possible electron sinks at the cathode including microbial growth and acetate conversion to microbial carbon storage molecules, which could reduce the gas recovery efficiency in MMCs [40,41]. In addition, it was recently reported that some metal ions such as iron and cobalt were deposited on the cathode surface in microbial electrosynthesis systems during operation [4]. Metal deposition could be one of the possible ways to increase current densities in the present study as well, given that several metal ions are present in the vitamin and mineral solutions added in the medium. Also, the liquid chemicals other than VFAs, such as methanol, was not measured in this study, which could further account for final products from CO_2 conversion [15]. Total cathodic recoveries from each biocathode were compared with data from the 4th cycle where the highest current was produced (Fig. 6B). Methane was a dominant bioproduct (20–25% of total cathodic recovery) from all Cu-based electrodes except for the Cu foil electrode, suggesting the success of conversion of electrons into methane in these reactors. Hydrogen was not efficiently converted into methane in Cu foil electrode MMCs, but there was a considerable production and recovery of formate (16 ± 9%), although the final concentration of formate was quite low (<0.25 mM). Formate recovery based on total coulombs was further increased in the last cycle (0–47% from each electrode; data not shown), possibly due to an unfavorable growth environment for methanogens as discussed above (i.e., 100% medium replenishment and washout of methanogens).

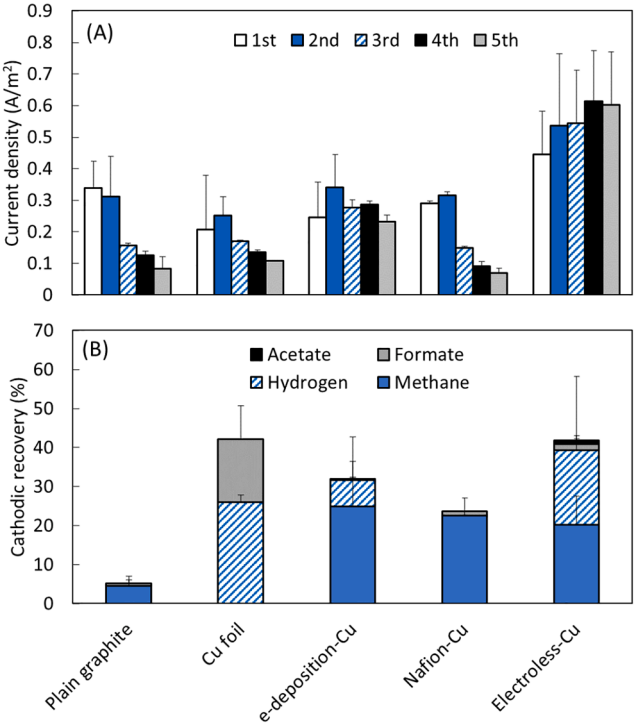

Fig. 6. (A) Average current densities normalized by cathode projected surface area during batch cycles 1–5 and (B) cathodic recovery at 4th batch cycle where the highest current was produced at fixed cathodic potential of –0.9 V vs. Ag/AgCl.

There was a large pH difference between the anolyte (5.8–6.2) and catholyte (7.6–8.2) in the electroless-Cu reactors where the highest current density was produced (Fig. 6A and Fig. S8). The pH difference may have increased further if the system was operated longer (>5 days). A high pH will adversely impact the growth of methanogens that have a relatively narrow optimal pH range (7.0–7.6) compared to acid-producing bacteria (5.0–8.5) [42,43]. It was recently shown that a pH imbalance can be reduced by using an anion exchange membrane in a more compact electrode design [44]. Similar configurations could be used to construct MMCs to avoid pH imbalances and improve long-term performance.

4. Conclusions

All copper-based cathodes except copper foil showed better MMC performance than plain graphite blocks, suggesting the potential of some forms of copper as a catalyst to increase methane production in biotic systems. The electroless-Cu was better than the other cathode materials in terms of CO_2-to-CH_4 conversion rate, current generation, and maintaining stability over multiple cycles without losing its methane production efficiency. The MMCs with Nafion-Cu cathodes had decreased performance over time possibly due to their hydrophobic surface and a non-uniform copper layer. Based on the overall results showing that some copper-based biocathodes could improve MMC performance, it may be possible to further improve performance though copper deposition onto more roughened or porous materials.

Declaration of Competing Interest

The authors declare that they have no known competing financial interests or personal relationships that could have appeared to influence the work reported in this paper.

Acknowledgement

This research was funded by the Stan and Flora Kappe endowment and other funds through The Pennsylvania State University.

Appendix A. Supplementary data

Supplementary data to this article can be found online at https://doi.org/10.1016/j.cej.2022.135076.

References

[1] R.W. Howarth, M.Z. Jacobson, How green is blue hydrogen? Energ. Sci. Eng. 9 (10) (2021) 1676–1687.
[2] M.-Y. Lee, K.T. Park, W. Lee, H. Lim, Y. Kwon, S. Kang, Current achievements and the future direction of electrochemical CO_2 reduction: A short review, Crit. Rev. Environ. Sci. Technol. 50 (8) (2020) 769–815.
[3] S. Cheng, D. Xing, D.F. Call, B.E. Logan, Direct biological conversion of electrical current into methane by electromethanogenesis, Environ. Sci. Technol. 43 (10) (2009) 3953–3958.
[4] B. Bian, L. Shi, K.P. Katuri, J. Xu, P. Wang, P.E. Saikaly, Efficient solar-to-acetate conversion from CO_2 through microbial electrosynthesis coupled with stable photoanode, Appl. Energ. 278 (2020), 115684.
[5] R.G. Grim, Z. Huang, M.T. Guarnieri, J.R. Ferrell, L. Tao, J.A. Schaidle, Transforming the carbon economy: challenges and opportunities in the convergence of low-cost electricity and reductive CO_2 utilization, Energ. Sci. Eng. 13 (2) (2020) 472–494.
[6] G. Baek, K.-Y. Kim, B.E. Logan, Impact of surface area and current generation of microbial electrolysis cell electrodes inserted into anaerobic digesters, Chem. Eng. J. 426 (2021), 131281.
[7] M. Lienemann, J.S. Deutzmann, R.D. Milton, M. Sahin, A.M. Spormann, Mediator-free enzymatic electrosynthesis of formate by the *Methanococcus maripaludis* heterodisulfide reductase supercomplex, Bioresour. Technol. 254 (2018) 278–283.
[8] G. Zhen, X. Lu, T. Kobayashi, G. Kumar, K. Xu, Promoted electromethanosynthesis in a two-chamber microbial electrolysis cells (MECs) containing a hybrid biocathode covered with graphite felt (GF), Chem. Eng. J. 284 (2016) 1146–1155.
[9] A. Ragab, K.P. Katuri, M. Ali, P.E. Saikaly, Evidence of spatial homogeneity in an electromethanogenic cathodic microbial community, Front. Microbiol. 10 (2019) 1747.
[10] M. Siegert, M.D. Yates, D.F. Call, X. Zhu, A. Spormann, B.E. Logan, Comparison of nonprecious metal cathode materials for methane production by electromethanogenesis, ACS Sust. Chem. Eng. 2 (4) (2014) 910–917.
[11] R. Blasco-Gómez, P. Batlle-Vilanova, M. Villano, M.D. Balaguer, J. Colprim, S. Puig, On the edge of research and technological application: a critical review of electromethanogenesis, Int. J. Mol. Sci. 18 (4) (2017) 874.
[12] A.J. Medford, A. Vojvodic, J.S. Hummelshøj, J. Voss, F. Abild-Pedersen, F. Studt, T. Bligaard, A. Nilsson, J.K. Nørskov, From the Sabatier principle to a predictive theory of transition-metal heterogeneous catalysis, J. Catal. 328 (2015) 36–42.
[13] A.B. Laursen, A.S. Varela, F. Dionigi, H. Fanchiu, C. Miller, O.L. Trinhammer, J. Rossmeisl, S. Dahl, Electrochemical hydrogen evolution: Sabatier's principle and the volcano plot, J. Chem. Educ. 89 (12) (2012) 1595–1599.
[14] K.P. Kuhl, T. Hatsukade, E.R. Cave, D.N. Abram, J. Kibsgaard, T.F. Jaramillo, Electrocatalytic conversion of carbon dioxide to methane and methanol on transition metal surfaces, J. Am. Chem. Soc. 136 (40) (2014) 14107–14113.
[15] K.P. Kuhl, E.R. Cave, D.N. Abram, T.F. Jaramillo, New insights into the electrochemical reduction of carbon dioxide on metallic copper surfaces, Energ. Environ. Sci. 5 (5) (2012) 7050–7059.
[16] S. Nitopi, E. Bertheussen, S.B. Scott, X. Liu, A.K. Engstfeld, S. Horch, B. Seger, I.E. L. Stephens, K. Chan, C. Hahn, J.K. Nørskov, T.F. Jaramillo, I.b. Chorkendorff, Progress and perspectives of electrochemical CO_2 reduction on copper in aqueous electrolyte, Chem. Rev. 119 (12) (2019) 7610–7672.
[17] J.G. Ferry, Fundamentals of methanogenic pathways that are key to the biomethanation of complex biomass, Curr. Opin. Biotechnol. 22 (3) (2011) 351–357.
[18] G. Baek, R. Rossi, P.E. Saikaly, B.E. Logan, The impact of different types of high surface area brush fibers with different electrical conductivity and biocompatibility on the rates of methane generation in anaerobic digestion, Sci. Tot. Environ. 787 (2021), 147683.
[19] M. Jiang, Y. Gao, S.A. Patil, H. Hou, W. Feng, S. Chen, Reactive coating modification of metal material with strong bonding strength and enhanced corrosion resistance for high-performance bioelectrode of microbial electrochemical technologies, J. Power Sour. 491 (2021), 229595.
[20] A. Baudler, I. Schmidt, M. Langner, A. Greiner, U. Schröder, Does it have to be carbon? Metal anodes in microbial fuel cells and related bioelectrochemical systems, Energ. Environ. Sci. 8 (7) (2015) 2048–2055.
[21] D.F. Call, B.E. Logan, A method for high throughput bioelectrochemical research based on small scale microbial electrolysis cells, Biosens. Bioelectron. 26 (11) (2011) 4526–4531.
[22] N. Aryal, L. Wan, M.H. Overgaard, A.C. Stoot, Y. Chen, P.-L. Tremblay, T. Zhang, Increased carbon dioxide reduction to acetate in a microbial electrosynthesis reactor with a reduced graphene oxide-coated copper foam composite cathode, Bioelectrochemistry 128 (2019) 83–93.
[23] Z. Shao, Y. Zhang, N. Zhang, J. Xia, Preparation and research of electroless copper on carbon fibers, Mater. Manuf. Processes 31 (1) (2016) 12–17.
[24] Y. Zhang, M.D. Merrill, B.E. Logan, The use and optimization of stainless steel mesh cathodes in microbial electrolysis cells, Int. J. Hydrogen Energ. 35 (21) (2010) 12020–12028.
[25] S. Siracusano, V. Baglio, A. Di Blasi, N. Briguglio, A. Stassi, R. Ornelas, E. Trifoni, V. Antonucci, A.S. Aricò, Electrochemical characterization of single cell and short stack PEM electrolyzers based on a nanosized IrO_2 anode electrocatalyst, Int. J. Hydrogen Energ. 35 (11) (2010) 5558–5568.
[26] M.C.A.A. van Eerten-Jansen, N.C. Jansen, C.M. Plugge, V. de Wilde, C.J. N. Buisman, A. ter Heijne, Analysis of the mechanisms of bioelectrochemical methane production by mixed cultures, J. Chem. Technol. Biotechnol. 90 (5) (2015) 963–970.
[27] M.C.A.A. Van Eerten-Jansen, A.B. Veldhoen, C.M. Plugge, A.J.M. Stams, C.J. N. Buisman, A. Ter Heijne, Microbial community analysis of a methane-producing biocathode in a bioelectrochemical system, Archaea 2013 (2013) 1–12.
[28] Z. Mao, Y.i. Sun, Y. Zhang, X. Ren, Z. Lin, S. Cheng, Effect of start-up process using different electrochemical methods on the performance of CO_2-reducing methanogenic biocathodes, Int. J. Hydrogen Energ. 46 (4) (2021) 3045–3055.
[29] G. Baek, J. Kim, S. Lee, C. Lee, Development of biocathode during repeated cycles of bioelectrochemical conversion of carbon dioxide to methane, Bioresour. Technol. 241 (2017) 1201–1207.
[30] L.e. Shi, S. Zhuo, M. Abulikemu, G. Mettela, T. Palaniselvam, S. Rasul, B.o. Tang, B. Yan, N.B. Saleh, P. Wang, Annealing temperature effects on photoelectrochemical performance of bismuth vanadate thin film photoelectrodes, RSC Adv. 8 (51) (2018) 29179–29188.
[31] M.H. Suliman, A. Adam, M.N. Siddiqui, Z.H. Yamani, M. Qamar, The impact of microstructural features of carbon supports on the electrocatalytic hydrogen evolution reaction, Catal. Sci. Technol. 9 (6) (2019) 1497–1503.
[32] X. Chen, Y. Li, X. Yuan, N. Li, W. He, J. Liu, Synergistic effect between poly (diallyldimethylammonium chloride) and reduced graphene oxide for high electrochemically active biofilm in microbial fuel cell, Electrochim. Acta 359 (2020), 136949.
[33] R. Rossi, D.M. Hall, L.e. Shi, N.R. Cross, C.A. Gorski, M.A. Hickner, B.E. Logan, Using a vapor-fed anode and saline catholyte to manage ion transport in a proton exchange membrane electrolyzer, Energ. Environ. Sci. 14 (11) (2021) 6041–6049.
[34] Y. Hori, A. Murata, R. Takahashi, Formation of hydrocarbons in the electrochemical reduction of carbon dioxide at a copper electrode in aqueous solution, J. Chem. Soc., Faraday Trans. 1 85 (8) (1989) 2309, https://doi.org/10.1039/f19898502309.
[35] Y. Yi, G. Weinberg, M. Prenzel, M. Greiner, S. Heumann, S. Becker, R. Schlögl, Electrochemical corrosion of a glassy carbon electrode, Catal. Today 295 (2017) 32–40.
[36] N. Aryal, F. Ammam, S.A. Patil, D. Pant, An overview of cathode materials for microbial electrosynthesis of chemicals from carbon dioxide, Green Chem. 19 (24) (2017) 5748–5760.
[37] J. Maruyama, I. Abe, Influence of anodic oxidation of glassy carbon surface on voltammetric behavior of Nafion®-coated glassy carbon electrodes, Electrochim. Acta 46 (22) (2001) 3381–3386.
[38] K. Guo, S. Freguia, P.G. Dennis, X. Chen, B.C. Donose, J. Keller, J.J. Gooding, K. Rabaey, Effects of surface charge and hydrophobicity on anodic biofilm formation, community composition, and current generation in bioelectrochemical systems, Environ. Sci. Technol. 47 (13) (2013) 7563–7570.
[39] M. Wang, L. Wan, J. Luo, Promoting CO_2 electroreduction on CuO nanowires with a hydrophobic Nafion overlayer, Nanoscale 13 (6) (2021) 3588–3593.
[40] S. Freguia, K. Rabaey, Z. Yuan, J. Keller, Electron and carbon balances in microbial fuel cells reveal temporary bacterial storage behavior during electricity generation Environ, Sci. Technol. 41 (8) (2007) 2915–2921.
[41] M. Cerrillo, M. Viñas, A. Bonmatí, Startup of electromethanogenic microbial electrolysis cells with two different biomass inocula for biogas upgrading, ACS Sust. Chem. Eng. 5 (10) (2017) 8852–8859.
[42] W. Fang, P. Zhang, G. Zhang, S. Jin, D. Li, M. Zhang, X. Xu, Effect of alkaline addition on anaerobic sludge digestion with combined pretreatment of alkaline and high pressure homogenization, Bioresour. Technol. 168 (2014) 167–172.
[43] M.H. Hwang, N.J. Jang, S.H. Hyun, I.S. Kim, Anaerobic bio-hydrogen production from ethanol fermentation: the role of pH, J. Biotechnol. 111 (3) (2004) 297–309.
[44] R. Rossi, G. Baek, P.E. Saikaly, B.E. Logan, Continuous Flow Microbial Flow Cell with an Anion Exchange Membrane for Treating Low Conductivity and Poorly Buffered Wastewater, ACS Sust. Chem. Eng. 9 (7) (2021) 2946–2954.